Electronic Supplementary Information

Ultrathin $HNbWO_6$ Nanosheets: Facile Synthesis and Enhanced Hydrogen Evolution Performance from Photocatalytic Water Splitting

Yuhao Liu, Jinhua Xiong, Shuiguang Luo, Ruowen Liang, Na Qin, Shijing Liang, Ling Wu**

State key laboratory of photocatalysis on energy and environment,

Fuzhou University, Fuzhou 350002, P. R. China

**Corresponding Author. E-mail: wuling@fzu.edu.cn*

Experimental Details

1. Material Synthesis.

1.1 Chemicals: All chemicals are analytical grade and used as received without further purification.

1.2 Preparation of monolayer $HNbWO_6$ nanosheets

Layered $HNbWO_6$ (L-$HNbWO_6$) was prepared by proton exchange of the precursors $LiNbWO_6$, which were obtained by calcinations stoichiometric amounts of WO_3, Nb_2O_5 and Li_2CO_3 at 1033 K for 48 h with one intermediate grinding. The proton-exchange reaction for the generation of layered $HNbWO_6$•$1.5H_2O$ was carried out in an aqueous solution of nitric acid (4 M) at a given temperature for six days. During the proton exchange reaction, the acid solution was replaced with a fresh one every two days. The $HNbWO_6$ sample was then washed thoroughly with distilled water and dried in air at 333 K. The $HNbWO_6$ nanosheets suspensions were rapidly obtained (N-$HNbWO_6$) by adding 80.0 mg layered $HNbWO_6$ into a certain amount of triethanolamine (TEOA) aqueous solution under continuous stirring, then translucent monolayer nanosheets suspensions were formed in just a few minutes. The traditional top-down exfoliation process (T-$HNbWO_6$) was achieved by reaction with tetrabutylammonium (TBA^+) cations. The TBA^+OH^- solution was added into 100 mL of distilled water containing 0.4 g of layered $HNbWO_6$ until the pH reached 9.5-10.0. The resultant solution was shaken for two weeks. The insertion of voluminous and hydrophobic TBA^+ cations expands and hydrates the interlayer spaces, resulting in the exfoliation of individual metal oxide sheets. The suspension was then centrifuged, and the supernatant solution containing the nanosheets was collected. The addition of a HNO_3 aqueous solution (1.0 M, 100 mL) to 100 mL of the nanosheets solution resulted in immediate aggregation of the nanosheets as a precipitate. The aggregated samples, $HNbWO_6$ nanosheets, were then rinsed three times with 100 mL of 0.5 M HNO_3 aqueous solution to remove TBA^+ and with a large amount of distilled water to remove HNO_3 and finally were dried at 333 K in a vacuum oven. The powdered N-$HNbWO_6$ nanosheets were synthesized via the same procedure as the T-$HNbWO_6$ aggregated prepared.

2. Characterizations

The as-prepared samples were characterized by powder X-ray diffraction (XRD) on a Bruker D8 Advance X-ray diffractometer operated at 40 kV and 40 mA with Ni-filtered Cu Kα irradiation (λ = 1.5406 Å). The data were recorded in a 2θ range of 3–60° with a step width of 0.01°. The Brunauer–Emmett–Teller (BET) surface area was measured with an ASAP2020M apparatus (Micromeritics Instrument Corp.). The morphologies of the products were examined by field-emission scanning electron microscopy at an accelerating voltage of 5 kV (Hitachi New Generation SU8010). Transmission electron microscopy (TEM) images, higher-resolution transmission electron microscopy (HRTEM) images, selected area electron diffraction (SAED) and energy-dispersive X-ray spectroscopy (EDX) were recorded using a JEOL model JEM2010 EX microscope at an accelerating voltage of 200 kV. A tapping-mode atomic force microscopy (AFM, Nanoscope Multimode IIIa, Veeco Instruments) with Si-tip cantilever was used to evaluate the morphology of the obtained nanosheets on the mica substrate. UV−vis diffuse reflectance spectra (UV−vis DRS) were obtained by a Cary 500 UV−vis−NIR spectrophotometer. The Mott−Schottky analysis was performed at a Zahner electrochemical workstation. The concentration of Pt in the suspension was detected by the Ultima2 ICP optical emission spectrometer. The Fourier transformed infrared spectra (FTIR) were carried out on a Nicolet 670 Fourier transforms infrared spectrometer. FTIR spectra of pure samples were collected with diluting with KBr. The spectra were registered after accumulation of 32 scans and a resolution of 4 cm^{-1}.

3. Photocatalytic Reaction

The photocatalytic H_2 evolution activity was evaluated in an airtight gas recirculation system equipped with an inner irradiation quartz reaction cell. Typically, 80.0 mL $HNbWO_6$ nanosheets dispersion (N-$HNbWO_6$) in-situ reaction with simulated sunlight without adding extra sacrificial reagents. For comparison, 80.0 mg restacked $HNbWO_6$ nanosheets (T-$HNbWO_6$) were re-dispersed in 10 vol. % TEOA aqueous solution. Different amount of Pt co-catalyst was loaded on the surface of nanosheets by the in-situ photodeposition method using $H_2PtCl_6 \bullet 6H_2O$ as the precursor.[1,2] The suspension was then thoroughly degassed to remove dissolved air and irradiated by a 300 W Xenon lamp (PLS-SXE300C, Perfectlight Co., Beijing). The irradiation wavelength in photocatalytic reactions was mainly at 300-700nm. The reactant solution was stirred and maintained at room temperature by a flow of cooling water during the photocatalytic reaction. The amount of evolved H_2 was detected by an online gas chromatograph (Shanghai Precision Scientific Instrument Co, Ltd, GC112A, TCD, Ar carrier). The apparent quantum yield (AQY) is also measured under the same photocatalytic reaction conditions. The incident light intensity of the 300 W xenon lamp is measured by SpectriLight ILT950. The total number of incident photons is measured using a calibrated silicon photodiode. The AQY is calculated according to the following equations:

$$AQY(\%)=\text{"Number of reacted electrons"} / \text{"Number of incident photons"} \times 100$$

$$=\text{"Number of evolved } H_2 \text{ molecules"} / \text{"Number of incident photons"} \times 100$$

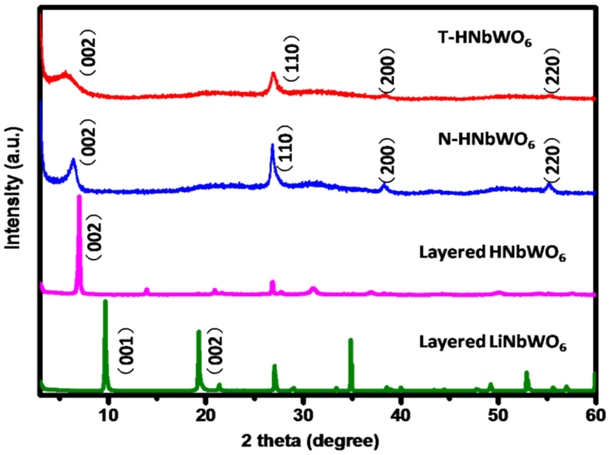

Fig. S1 XRD patterns of prepared $LiNbWO_6$, L-$HNbWO_6$, restacked T-$HNbWO_6$ and N-$HNbWO_6$ nanosheets.

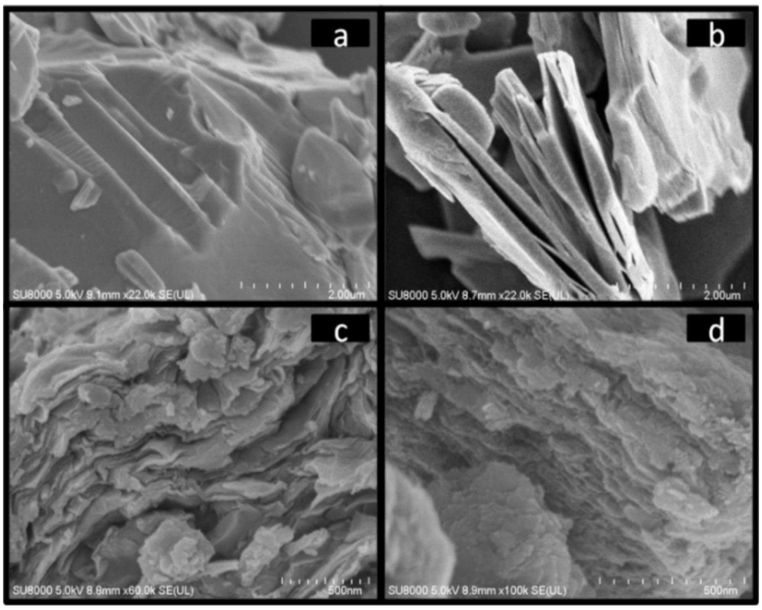

Fig. S2 SEM images of (a) $LiNbWO_6$, (b) L-$HNbWO_6$, (c) restacked N-$HNbWO_6$, nanosheets and (d) T-$HNbWO_6$ nanosheets.

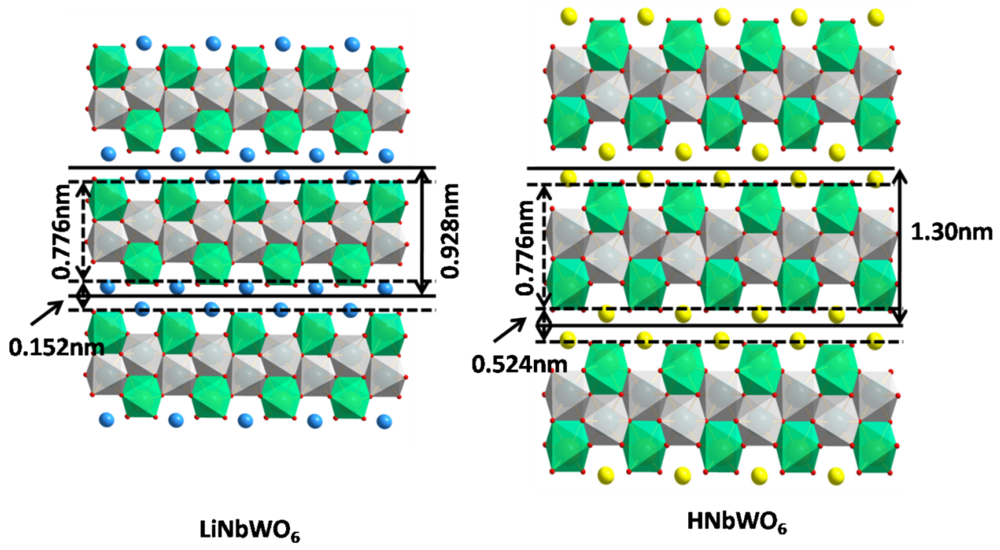

$LiNbWO_6$ $HNbWO_6$

Fig. S3 The theoretical calculation of the slab thickness and interlayer distance between $LiNbWO_6$ and $HNbWO_6$.

From Fig S3 left, we can conclude the slab thickness of the $LiNbWO_6$ is 0.928-2*0.076=0.776 nm. Assumed that the slab thickness is constant before and after the proton exchange reaction, the hydration layer spacing of $HNbWO_6$ can be calculated 1.30-0.776=0.524 nm (Fig. S3 right). Therefore, the thickness of bilayer is at least 0.776*2+0.524=2.076 nm. Due to the experimental height of $HNbWO_6$ nanosheets from AFM is between 1.8 and 2.0 nm, we can speculate the $HNbWO_6$ nanosheet prepared by this method is monolayer.

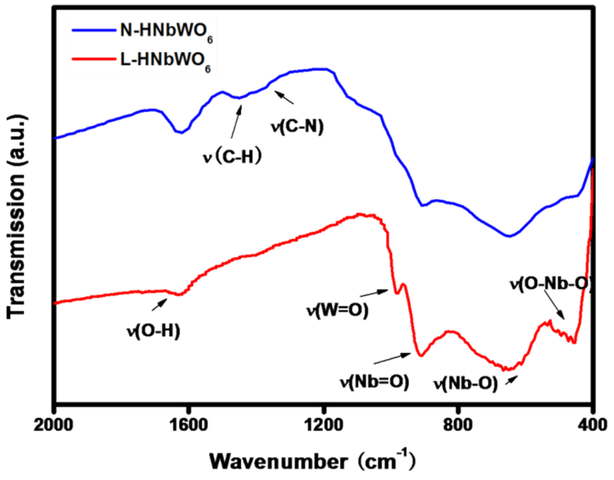

Fig. S4 FTIR spectra of layered $HNbWO_6$ and N-$HNbWO_6$ nanosheets.

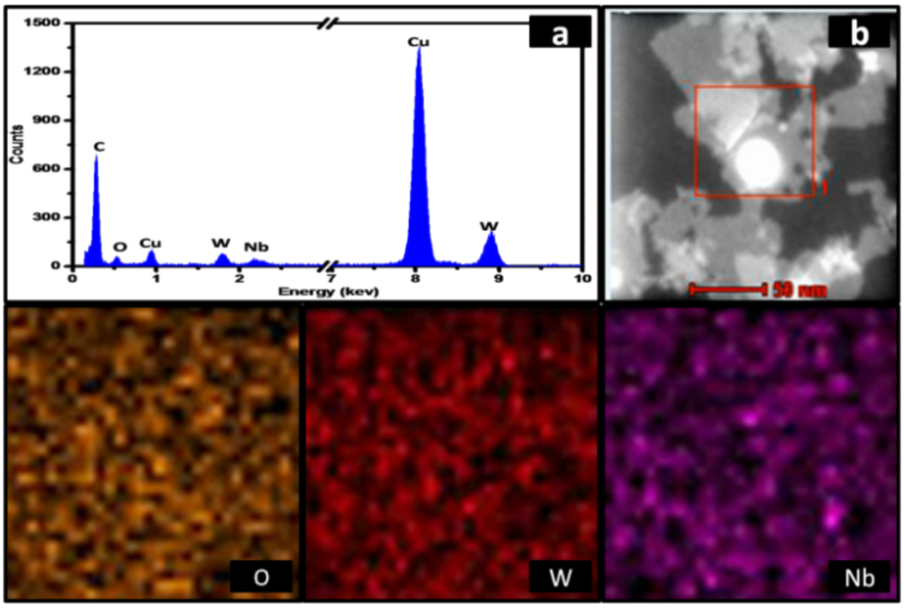

Fig. S5 (a) EDX spectrum and (b) mapping results of N-$HNbWO_6$ nanosheets.

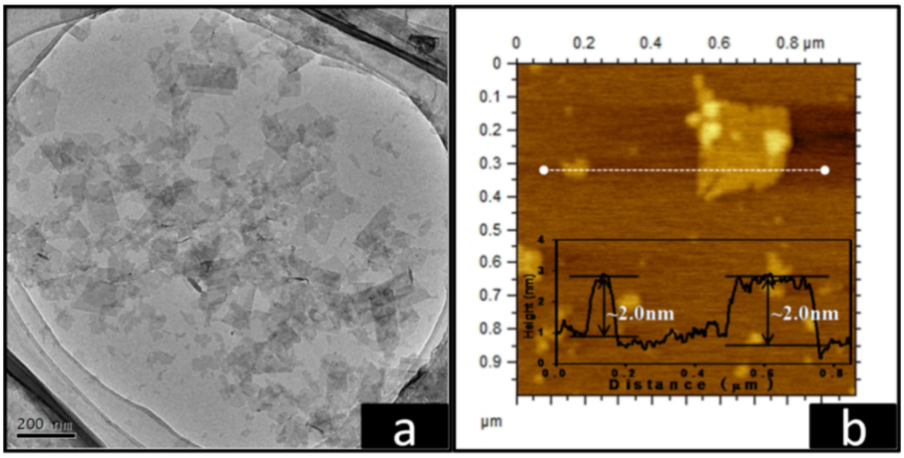

Fig. S6 TEM (a) and AFM (b) of $HNbWO_6$ nanosheets suspensions prepared by traditional method with TBAOH aqueous solution.

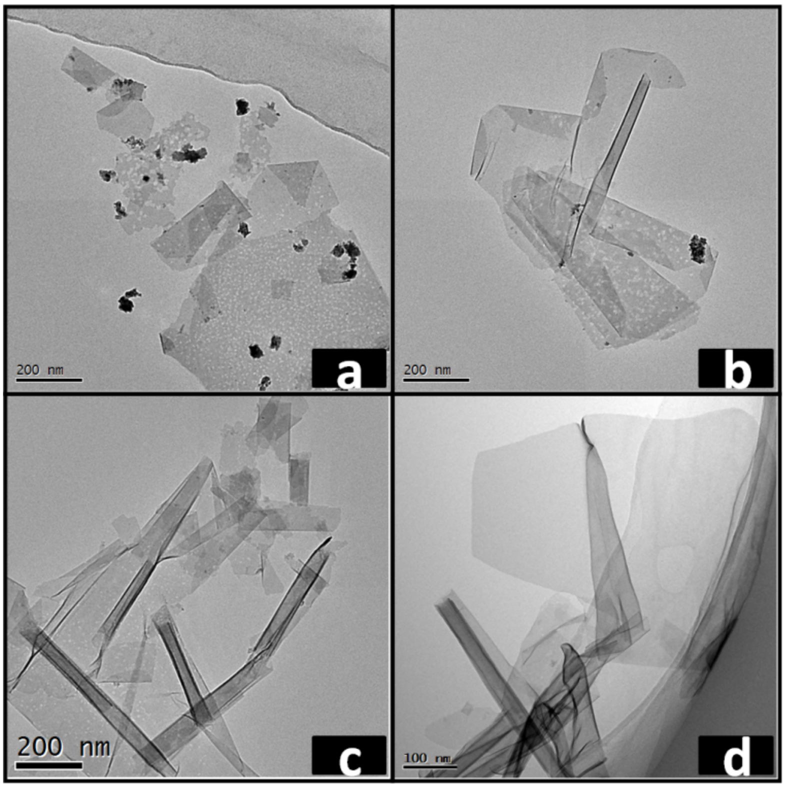

Fig. S7 TEM of $HNb_xTa_{1-x}WO_6$ nanosheets prepared with TEOA aqueous solution. (a) x = 0.7, (b) x = 0.5, (c) x = 0.3, (d) x = 0.

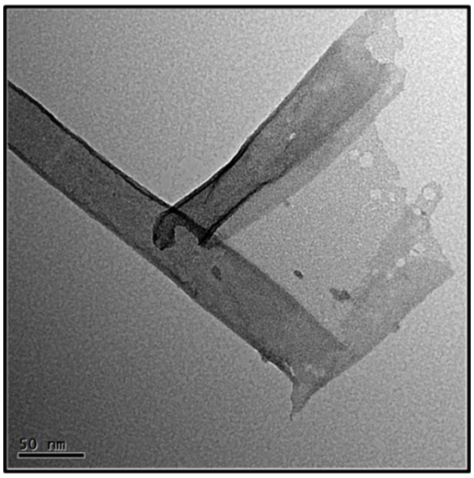

Fig. S8 TEM of $HNbWO_6$ nanosheets obtained with Triisopropanolamine (TIPA) aqueous solution.

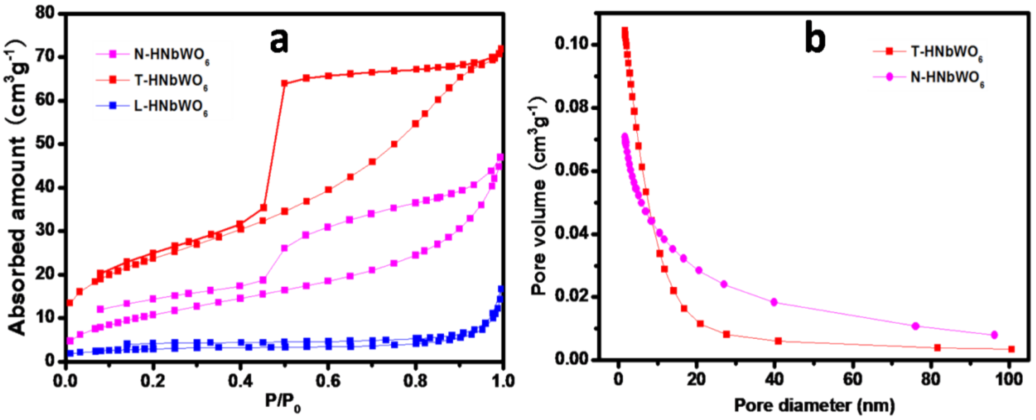

Fig. S9 N_2 adsorption-desorption isotherms (a) of restacked N-$HNbWO_6$ and T-$HNbWO_6$ nanosheets and its layered parent, (b) The pore size distribution curve of restacked N-$HNbWO_6$ and T-$HNbWO_6$ nanosheets.

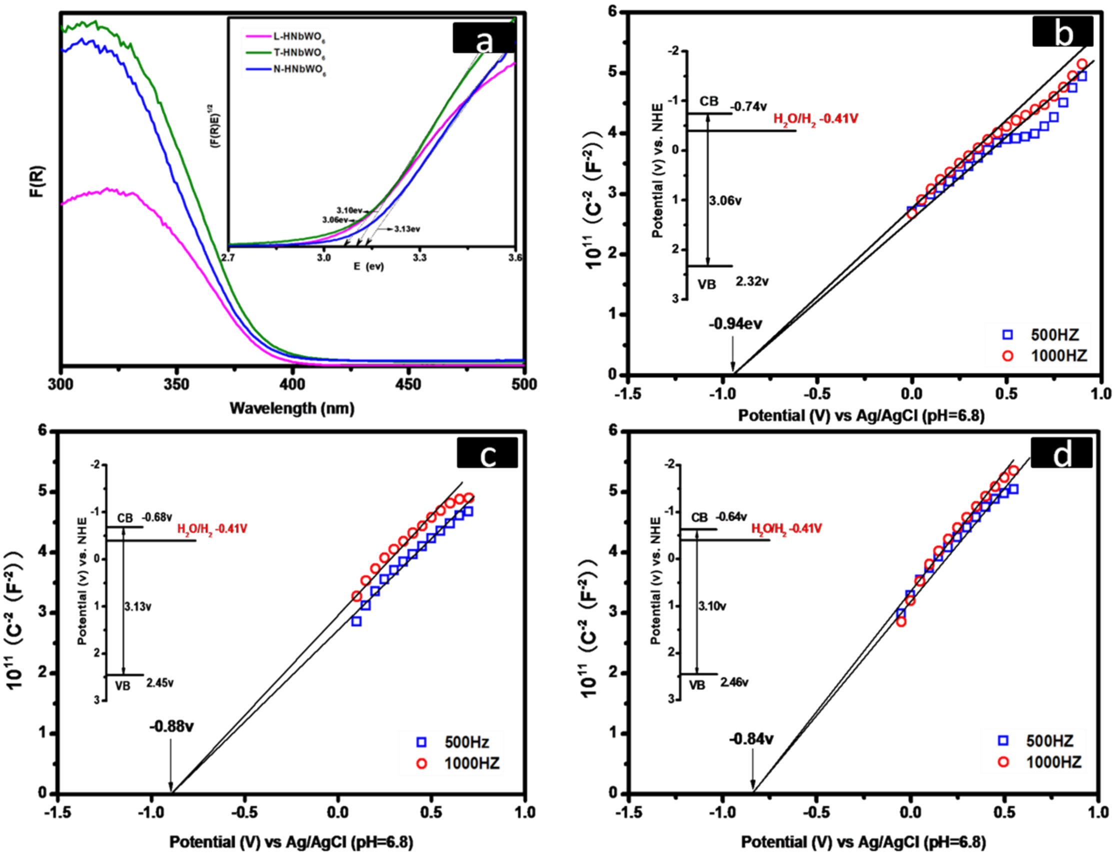

Fig. S10 (a) UV-Vis diffuse reflective spectra of L-$HNbWO_6$, restacked N-$HNbWO_6$ and T-$HNbWO_6$ nanosheets. Typical Mott−Schottky plots of L-$HNbWO_6$ (b), restacked N-$HNbWO_6$ (c) and T-$HNbWO_6$ (d) nanosheets in 0.2 M Na_2SO_4 aqueous solution (pH= 6.8).

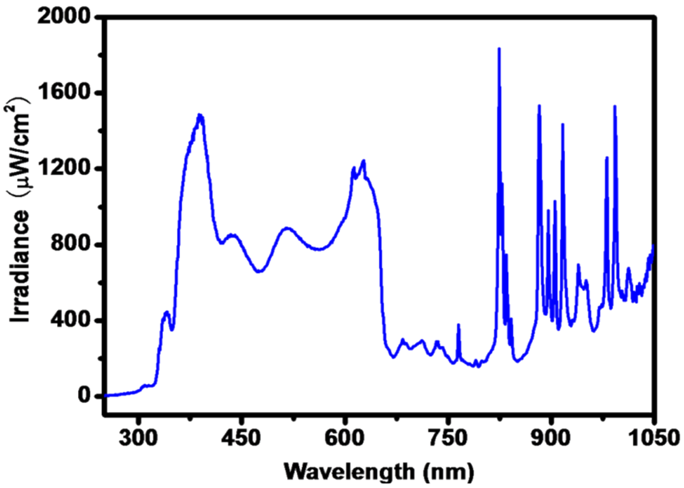

Fig. S11 Irradiance spectra of 300W xenon lamp.

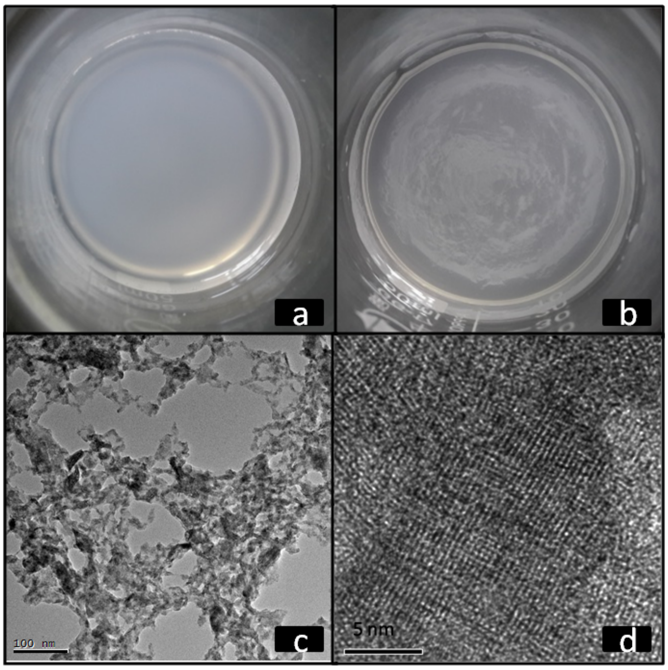

Fig. S12 Photograph of (a) $HNbWO_6$ ultrathin nanosheets dispersions obtained by acid–base reaction and (b) restacked T-$HNbWO_6$ nanosheets aggregates in the TEOA aqueous solution. (c) TEM and (d) HRTEM of restacked T-$HNbWO_6$ nanosheets.

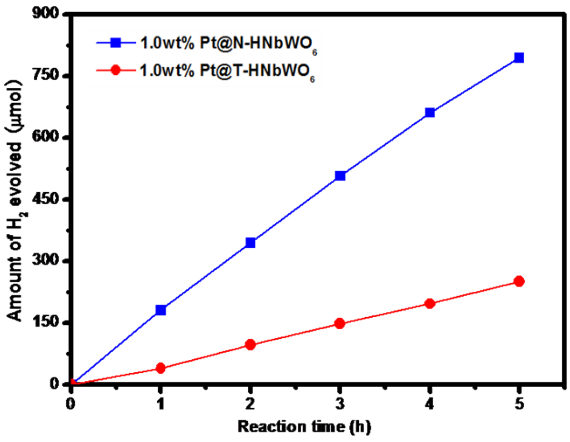

Fig. S13 Time course of H_2 evolved from water splitting using N-$HNbWO_6$ and T-$HNbWO_6$ nanosheets.

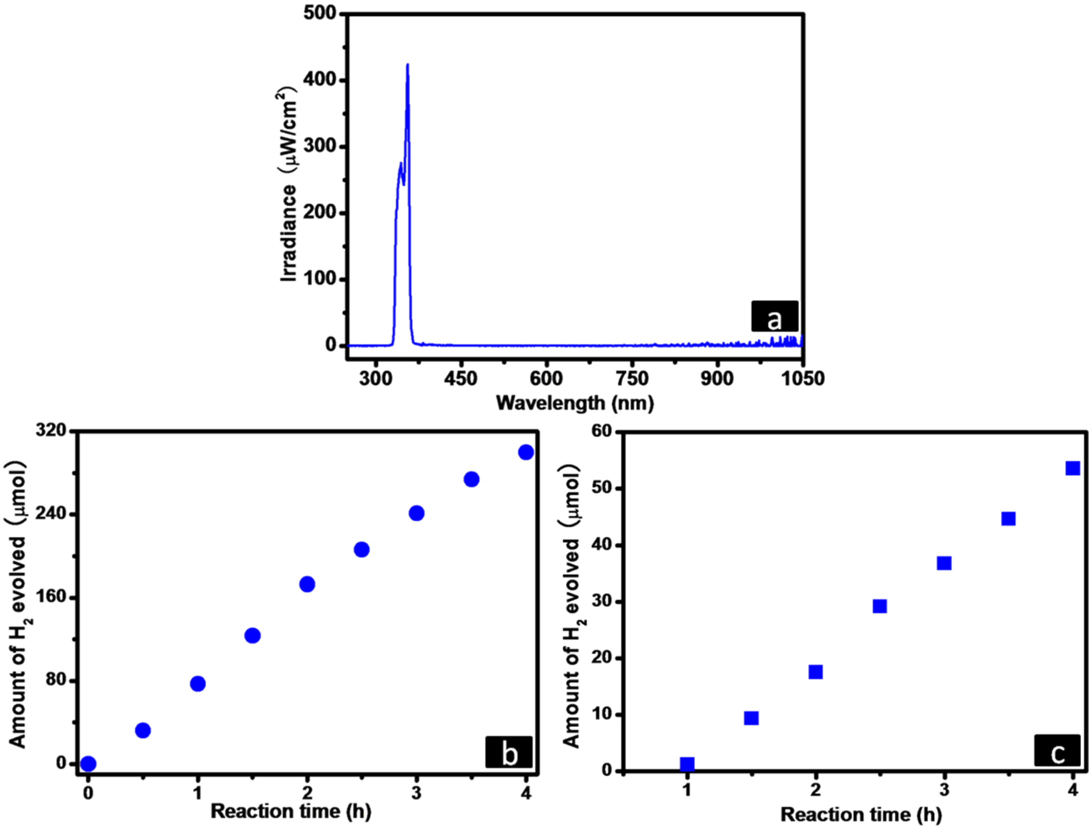

Fig. S14 Irradiance spectra of 300 W xenon lamp with a band-pass filter (λ=350±10 nm) (a). Time course of H_2 evolution on 1.0 wt% Pt loaded N-$HNbWO_6$ (b) and T-$HNbWO_6$ (c) under 300 W xenon lamp with a band-pass filter (λ = 350 nm).

Number of reacted electrons of N-$HNbWO_6$=74.6 μmol/h$\times10^{-6}\times2\times6.02\times10^{23}\div3600$ =2.49×10^{16} s^{-1}.

Number of reacted electrons of T-$HNbWO_6$=12.5 μmol/h$\times10^{-6}\times2\times6.02\times10^{23}\div3600$ =4.18×10^{15} s^{-1}.

Number of incident photons= 1.763×10^{17} s^{-1}.

AQY(%) (N-$HNbWO_6$)= 14.1%

AQY(%) (T-$HNbWO_6$)= 2.4 %

References

1. G. Zhang, M. Zhang, X. Ye, X. Qiu, S. Lin and X. Wang, *Adv. Mater.*, 2014, **26**, 805-809.
2. K. Maeda, M. Eguchi and T. Oshima, *Angew. Chem. Int. Ed.*, 2014, **53**, 13164-13168.